A&A 476, 675–684 (2007)
DOI: 10.1051/0004-6361:20077929

Astronomy & Astrophysics

Continuum emission in the 1–2000 Å range

E. Landi

Artep, Inc. at Naval Research Laboratory, 4555 Overlook Ave. S.W., 20375-5320, Washington DC, USA
e-mail: landi@poppeo.nrl.navy.mil

Received 22 May 2007 / Accepted 2 October 2007

ABSTRACT

Context. Continuum emission is a fundamental component of the solar and stellar spectra between 1 Å and 2000 Å and has important applications to plasma diagnostics. However, the importance of X-ray free-bound continuum radiation has been overlooked in recent years, and no assessment of the accuracy of different data and approximations underlying the calculation of continuum emissivity has been carried out to understand the reliability of diagnostic results.
Aims. The importance of free-bound radiation in the X-rays will be demonstrated and its effects on plasma diagnostics will be discussed. The importance of user-chosen parameters such as ion and element abundances, necessary to the calculation of continuum emissivity, will be assessed. The uncertainties in the atomic data underlying continuum calculations will be investigated.
Methods. We will use the CHIANTI spectral code to investigate the relative importance of the free-free, free-bound and two-photon radiation as a function of wavelength in the 1−2000 Å spectral range, and to assess the effects of user-chosen parameters on the calculation of the continuum emission. A comparison between continuum emissivity of two of the most widely used spectral codes, developed using very different atomic data and approximations, will give us an indication of their reliability.
Results. The effects of element abundances and of the neglect of free-bound radiation in the X-rays are shown to be significant, with important consequences for plasma diagnostics results. The total continuum emissivities of the two spectral codes we compared are found to be in agreement to better than 40% at all wavelengths and temperatures of interest, with only a few exceptions.

Key words. atomic processes – atomic data – Sun: UV radiation – Sun: X-rays, gamma rays – Sun: abundances – stars: abundances

1. Introduction

The calculation of X-ray, EUV and UV continuum emission from optically thin astrophysical plasmas in the 1−2000 Å wavelength range has always been of great importance for the analysis of the observed spectrum of the Sun and of other extrasolar objects. Continuum emission is very important in several spectral ranges at high temperatures and can be a major contributor to the energy losses of an optically thin plasma. Also, continuum emission can be used as a tool to measure the absolute element abundances, the emission measure, and the temperature in astrophysical plasmas.

The processes that produce the continuum emission below 2000 Å in the Sun and in cool stars are free-free (or *Bremsstrahlung*), free-bound (or *recombination*) and two-photon radiation. In the recent past, continuum emission has seen a revival of interest thanks to the recent missions RHESSI (Lin et al. 2002, working in the X-rays), RESIK (Sylwester et al. 2005, also working in X-rays) and SOHO/SUMER (Wilhelm et al. 1995, working in UV), whose observations of the solar continuum have allowed detailed temperature, emission measure and abundance diagnostics of the solar corona (e.g. Phillips et al. 2003, 2006; Sylwester et al. 2006; Phillips 2004; Landi et al. 2007; Feldman et al. 2003, 2004, 2005).

Plasma diagnostics involving continuum emission requires the use of several approximations, accurate atomic data and user-chosen parameters such as ion and element abundances in the emitting plasmas. However, to the best of our knowledge no systematic assessment of the importance for plasma diagnostics of such atomic data and approximations has been done. Such an assessment is one aim of the present paper.

It has become standard thinking that the X-ray continuum emission in the 1−10 Å wavelength range in solar and stellar flares is dominated by free-free emission, with the free-bound radiation providing only a limited contribution that could even be neglected, especially at shorter wavelengths. Here we also argue that free-bound emission plays a crucial role in the continuum emission in the 1−10 Å range at most temperatures of astrophysical interest, and that its parameters need to be carefully considered before any attempt is made at using the observed X-ray total continuum to measure the physical properties of active and flaring plasmas.

We will make use of the continuum model available in the CHIANTI spectral code (Dere et al. 1997; Landi et al. 2006, described briefly in Sect. 2) to predict the free-free and free-bound emissivity in the X-rays and demonstrate the importance of the latter for the X-ray continuum (Sect. 3), and to assess the effects of user-defined parameters such as ion fractions and element abundances on continuum emission in the 1−2000 Å range (Sect. 4). We will compare the results from the CHIANTI and Mewe et al. (1986, hereafter MEWE, also described in Sect. 2) codes in order to assess the effects of very different atomic data and approximations on the calculated continuum (Sect. 5). The effects of user-defined parameters and of differences in approximations and atomic data on plasma diagnostic results obtained with continuum emission are discussed in Sect. 6. The results are summarized in Sect. 7.

2. Tools: continuum models

2.1. CHIANTI continuum model

Continuum radiation was first included in CHIANTI as part of version 2 of the database (Landi et al. 1999), but was changed in both version 3 (Dere et al. 2001) and 4 (Young et al. 2003). Version 5 (Landi et al. 2006), which is used here, did not bring any changes to the continuum calculation.

Version 2 was limited to adopting the Gronenschild & Mewe (1978) approach, with the only difference that collisional depopulation of the metastable levels was taken into account in the two-photon emission by calculating explicitly the level populations of each ion solving the equations of statistical equilibrium. Version 3 improved on it by including more recent Gaunt factors for the free-free radiation from Sutherland (1998), and by changing the free-bound calculation to adopt the approach of Rybicki & Lightman (1979), setting the Gaunt factors to unity and using the energy levels already in the CHIANTI database in the calculation. Version 4 completely revised the way continuum radiation is calculated, improving over the previous versions as described below.

2.1.1. Free-free continuum

CHIANTI uses the same approach as Mewe & Gronenschild (1978) to calculate the free-free continuum emission, but the Gaunt factors used in version 5 are more recent and accurate than those from Karzas & Latter (1961) used by the Mewe & Gronenschild (1978) model. The relativistic thermal bremsstrahlung Gaunt factors from Itoh et al. (2000) are used by CHIANTI for temperatures in the $6.0 \leq \log T_{\rm e} \leq 8.5$ range and wavelengths in the $-4.0 \leq \log(hc/\lambda kT_{\rm e}) \leq -1.0$ range; outside these ranges, the non-relativistic Gaunt factors of Sutherland (1998) are used.

In the calculation, ion and element abundances are chosen interactively by the user among several different available datasets.

2.1.2. Free-bound continuum

CHIANTI calculates the free-bound continuum emission (in erg cm^{-3} s^{-1} Å^{-1}) for recombination from the ground level of an ion X^{+m+1} to the ground as well as into the excited levels of an ion X^m, as

$$\frac{{\rm d}P_{\rm fb}}{{\rm d}\lambda} = 3.0992\times10^{-52}N_{\rm e}N\left(X^{+m+1}\right)\frac{E^5}{T^{3/2}}\sum_i\frac{\omega_i}{\omega_0}\sigma_i^{\rm bf}{\rm e}^{-\frac{E-I_i}{kT}} \quad (1)$$

where $N\left(X^{+m+1}\right)$ is the number of recombining ions X^{+m+1} per unit volume, E is the energy (in cm^{-1}) of the radiation at wavelength λ, ω_i and ω_0 are the statistical weights of level i of the recombined ion and of the ground level of the recombining ion respectively, $\sigma_i^{\rm bf}$ is the photoionization cross section from level i of the recombined ion to the ground level of the recombining ion (in units of 10^{-18} cm^{-2}) and I_i is the ionization energy (in cm^{-1}) of level i.

The photoionization cross-sections from the ground level of the recombined ion are taken from the analytical fits of Verner & Yakovlev (1995), while those for photoionization from the excited levels are calculated using the hydrogenic approximation as

$$\sigma_i^{\rm bf} = 0.1075812\frac{I_i^2 g_{\rm bf}}{n_i E^3} \quad (2)$$

where $g_{\rm bf}$ is the bound-free Gaunt factor from Karzas & Latter (1961), and n_i is the principal quantum number of the ejected electron. It is important to note that no Gaunt factor is involved in the free-bound emission from the ground level.

In CHIANTI, data for recombination continuum are included for all the ions in the database, plus several ions for which CHIANTI does not calculate line emissivities, including all neutral species of the most abundant elements in the universe. (nl)-resolved energy levels are considered for all ions, whose energies are taken from CHIANTI or from the literature.

In the calculation, ion and element abundances are chosen interactively by the user among several different available datasets.

2.1.3. Two-photon continuum

The two-photon emissivity is calculated by CHIANTI including H-like and He-like ions up to Ni, by summing the contribution of each individual ion given by

$$\frac{{\rm d}P_{2p}}{{\rm d}\lambda} = \frac{hc}{4\pi\lambda}A_{ji}N_j(X^{+m})\phi\left(\frac{\lambda_0}{\lambda}\right) \quad (3)$$

where λ_0 and A_{ji} are the transition's wavelength and Einstein spontaneous emission coefficient, $\phi\left(\frac{\lambda_0}{\lambda}\right)$ is the spectral distribution and $N_j(X^{+m})$ is the population of the metastable level (1s2s $^2{\rm S}_{1/2}$ in H-like ions, 1s2s $^1{\rm S}_0$ in He-like ions) from which the two-photon transition is generated. The main features of this model lie in the accuracy of the data for the A values, and in the $N_j(X^{+m})$ level population, obtained by solving the system of equations for the statistical balance within each ion considering all relevant population and de-population processes. In this way, collisional depopulation of the metastable level is directly taken into account using collision rates and dispensing from the use of approximate Gaunt factors for collisional excitation. The data used for the H-like and He-like sequences are described in Young et al. (2003). CHIANTI calculates the two-photon continuum at all wavelength ranges.

The importance of directly taking into account the electron density is shown in Fig. 1 for H and He. In the low-density limit the two-photon continuum from H I at wavelengths longer than 1215.6 Å can be very strong and even dominate the other continua, but as the electron density becomes larger than 10^8 cm^{-3} it starts to decrease due to collisional depopulation of the metastable 2s $^2{\rm S}_{1/2}$ level from which it originates. The same applies to the two-photon continua from He, although their emissivity is lower than that of hydrogen. However, it is to be noted that the simple collisional-radiative model adopted by CHIANTI to calculate the level populations of H I, He I and He II is inadequate and could result in inaccuracies in the populations of the metastable level since it neglects other processes that might be involved in populating and de-populating the metastable level. The magnitude of these inaccuracies is difficult to assess since the formation of the line intensities of these ions is still under debate. At coronal densities collisional excitation, however, should be sufficient to limit the role of the other processes.

For all other ions in the CHIANTI database density effects are negligible at $\log N_{\rm e} \leq 12$. In the calculation, ion and element abundances are chosen interactively by the user from several different available datasets.

2.2. MEWE continuum model

The MEWE continuum model, available in *SolarSoft* with the widely used IDL computer program *conflx.pro*, is thoroughly

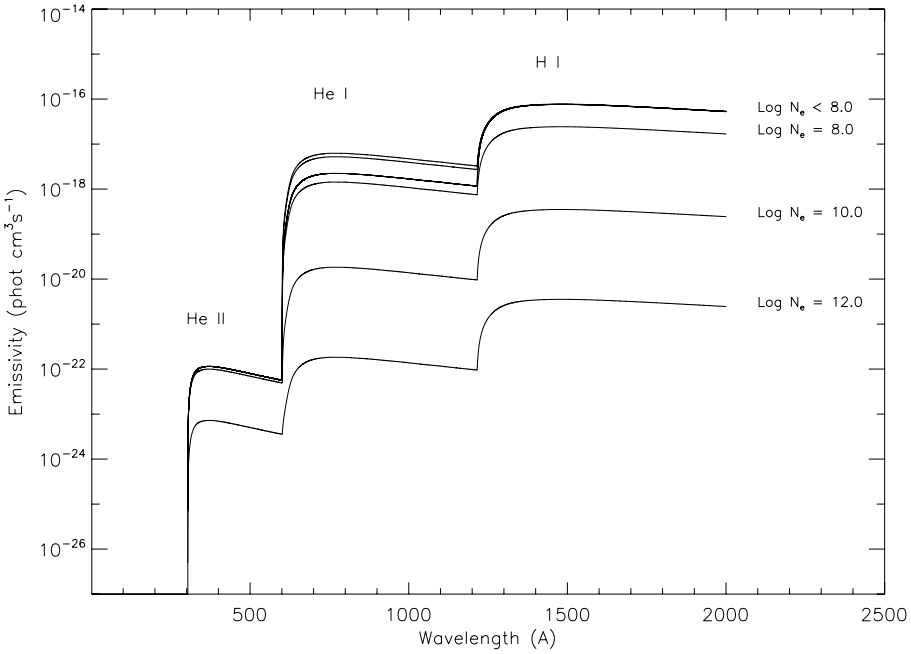

Fig. 1. Two-photon emissivity below 2000 Å, calculated assuming $\log T_e = 4.3$ and several values of the electron density. The emission is due, in order of increasing wavelength, to He II, He I and H I.

described in Mewe et al. (1986) and Gronenschild & Mewe (1978). Here we limit ourselves to overview the main features of this model and its implementation in the freely available and commonly used program *conflx.pro*.

The MEWE continuum model is based on a non-relativistic calculation of the free-free, free-bound and two-photon radiation, and is limited to the 1−1000 Å spectral range; the two-photon continuum is calculated only in the 19−200 Å range and is assumed to be negligible outside those wavelengths. The total continuum energy emissivity at wavelength λ (in erg cm^{-3} s^{-1} Å^{-1}) was given by Mewe et al. (1986) to be

$$P_c = 2.051 \times 10^{-22} N_e^2 G_c \frac{e^{-\frac{143.9}{\lambda T}}}{\lambda^2 T_e^{1/2}} \quad (4)$$

where N_e and T are the electron density and temperature, respectively, λ is the wavelength (in Å), and the temperature T is given in MK. The *total Gaunt factor* G_c was defined as

$$G_c = G_{ff} + G_{fb} + G_{2\gamma} \quad (5)$$

where G_{ff} is the free-free Gaunt factor, G_{fb} is the free-bound Gaunt factor, and $G_{2\gamma}$ is the two-photon Gaunt factor. The expressions for each of these Gaunt factors are given in Mewe et al. (1986) and will not be repeated here. Several approximations were adopted in the derivation of the Gaunt factors of each individual continuum process.

2.2.1. Free-free continuum

The temperature-averaged Gaunt factors from Karzas & Latter (1961) were adopted to calculate the free-free Gaunt factor G_{ff} and were approximated by an analytic formula whose coefficients were optimized to reproduce the Karzas & Latter (1961) Gaunt factors within 10% in the 1−1000 Å wavelength range and in the 10^5−10^8 K temperature range. The ions were assumed to be hydrogenoid and always in the ground state.

2.2.2. Free-bound continuum

The free-bound Gaunt factor was approximated by considering radiative recombinations into hydrogenic ions, taking into account both recombination to the ground and to the excited levels. Gronenschild & Mewe (1978) noted that the Karzas & Latter (1961) Gaunt factors g_{fb} for radiative recombination were in the 0.8−1.0 range, so Mewe et al. (1986) approximated them by adopting $g_{fb} = 0.9$ for recombination into the ground state and $g_{fb} = 1.0$ for recombination into excited states. Excited states are grouped in one single state with principal quantum number $n = n_0 + 1$ where n_0 is the principal quantum number of the ground level.

2.2.3. Two-photon continuum

The two-photon Gaunt factor was calculated including H-like and He-like systems, by approximating the collisional excitation from the ground level to the metastable level that originates the two-photon transition with the average excitation Gaunt factor $\bar{g}$ and the absorption oscillator strength f. The values of f and $\bar{g}$ were given by Mewe et al. (1986). The two-photon spectral decay distribution was approximated with an analytical formula with accuracy within 4% to 14%. Gronenschild & Mewe (1978) also showed that collisional depopoulation of the metastable level was negligible at densities typical of the solar coronae and of supernova remnants.

2.2.4. Implementation

The equations given in Mewe et al. (1986) were used to calculate the total Gaunt factors and the continuum emission. The resulting total Gaunt factors were fitted with analytical formulae to provide a simple set of equations which could be implemented in a computer program which allowed users to calculate in a very short time the continuum emission for wide ranges of temperature and wavelength. Such analytical formulae constitute the core of the *conflx.pro* routine available in *SolarSoft*. In such a fit, the two-photon continuum was included only in the 19−200 Å range, where it is strongest due to the emission from C, N and

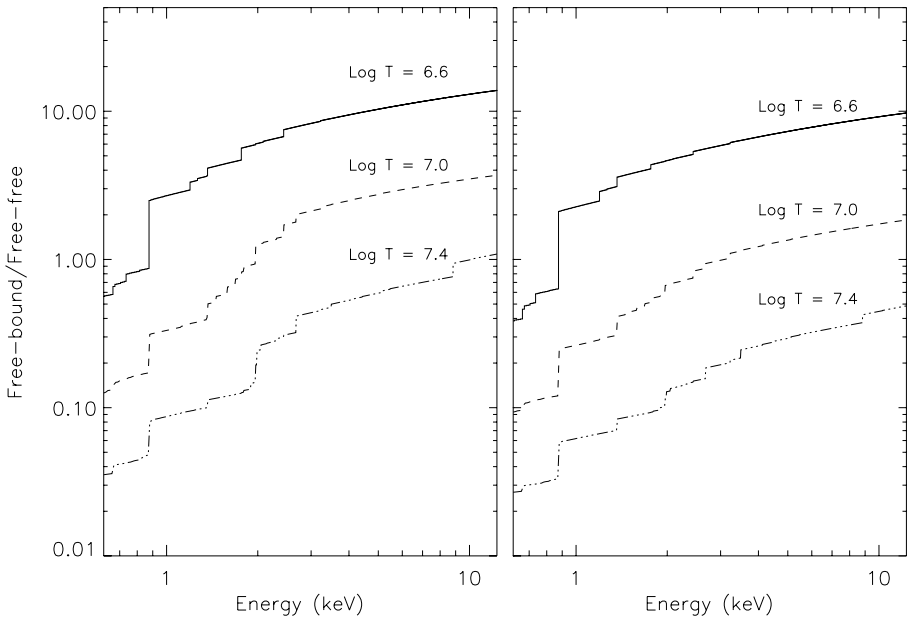

Fig. 2. Ratio between the free-bound and the free-free continua in the X-ray range between 0.6 and 12.3 keV (corresponding to the 1−20 Å wavelength range). Temperatures are typical of solar and stellar flares. *Left*: coronal abundances; *right*: photospheric abundances.

O. Also, only a limited number of recombination edges were included in the fit (around 16, corresponding to the edges of ions of some of the most abundant elements).

The Gaunt factors for free-free, free-bound and two-photon radiation all depend on the element and ion abundances. Mewe et al. (1986) used the Allen (1973) cosmic abundances and the Arnaud & Rothenflug (1985) ion fractions (the best available at the time) to calculate the Gaunt factors to be fitted with analytical formulae.

By fitting the resulting continuum emissivities, Mewe et al. (1986) made it impossible to change the ion and element abundances included in the continuum emission calculation. While this approach is practical because it provides a very fast routine, it may cause problems in plasma diagnostics in the event that the element abundances of the emitting plasma depart from the adopted values. This point will be discussed in more detail in Sect. 4.

3. Relative importance of different continua

The relative strength of the free-free, free-bound and two-photon continua depends on both wavelength and temperature.

3.1. 1–20 Å range

In the soft X-ray range, between 1 Å and 20 Å, the free-bound continuum dominates the emission at all wavelengths up to temperatures of $\log T_e \simeq 6.2$. The free-free and free-bound continua are comparable in the $6.4 \leq \log T_e \leq 7.4$, and their relative strength depends on the wavelength (or energy) because of the presence of the recombination edges as shown in Fig. 2, where the ratio between the free-bound and the free-free radiation is displayed: below each recombination edge (whose presence causes the jumps in the ratios displayed in Fig. 2), free-free and free-bound continua have a very similar wavelength (or energy) dependence. The relative strength of free-free and free-bound continua also depends on the element abundance and the temperature: the larger the element abundance is, the stronger the free-bound radiation over the free-free, while the ratio between free-bound and free-free continua decreases approximately linearly with temperature. For $\log T_e \geq 7.6$ the free-free emissivity largely dominates the 1−20 Å wavelength range (see Fig. 2). The two-photon continuum is always less important than the other two continua.

Figure 2 demonstrates that the free-bound radiation cannot be neglected in the 1−20 Å range.

3.2. 20–2000 Å range

In the 20–2000 Å range the free-bound emission from H I and He II dominates the continuum spectrum up to one million K, with the relative strength of the free-free overtaking the free-bound as the temperature increases. The differences are strongly wavelength dependent due to the presence of the recombination edges, so that at longer wavelengths the free-free continuum reaches the free-bound at lower temperatures. The free-free continuum completely dominates the spectrum at temperatures larger than $\log T_e \simeq 6.6$.

The two-photon continuum is predicted to be significant, or even dominant, on two occasions. At coronal temperatures, in the $5.6 \leq \log T_e \leq 6.6$, two-photon continuum from H-like and He-like C, N and O ions provide significant or even dominant contributions to the total continuum; its importance is maximum in the 20−40 Å range, but still significant up to ≃80 Å. At low temperatures ($\log T_e \leq 5.4$) two-photon emission from H I and He II can be important at certain wavelength ranges if the density is low enough: for $\log T_e \leq 4.4$ H I emission is strong at wavelengths larger than 1215 Å, while in the $4.6 \leq \log T_e \leq 5.4$ range the He II emission is emitted in the 300−700 Å range. The comparison with the solar spectrum in the 500−1600 Å from the SOHO/SUMER atlas observed by Curdt et al. (2001) on the disk shows no trace of a rise in the observed continuum corresponding to the H I two-photon emission. This might be due to different physical conditions in the solar plasma from those assumed in the present calculations (especially for the electron density), and to additional population and depopulation processes of H I levels active in the solar lower atmosphere that are not accounted for in CHIANTI.

4. Effects of user-defined parameters

In the calculation of the continuum it is necessary to adopt a set of ion abundances and element abundances. This choice may have important effects on the final results, which we investigate here using the latest version of the CHIANTI database, since the *conflx.pro* routine using the MEWE approach does not allow these parameters to be changed.

4.1. Ion abundances

The effects of different ion abundances were studied by comparing the free-free, free-bound and two-photon continuum emissivities calculated adopting the Arnaud & Rothenflug (1985) and the Mazzotta et al. (1998) ion fractions.

The effects on the free-free emission are lower than 5% at all temperatures except below 20 000 K, where some differences in the ion abundances of H I cause the differences to be up to 35%; however, at these temperatures the free-free continuum emission is negligible.

The effects on the free-bound and two-photon continua are usually within 10%, except in the few wavelength regions and at the few temperatures where the free-bound continuum is dominated by recombination (or two-photon emission) from an ion with abundance smaller than 10^{-3}. In these cases, differences can be very high because the ion fraction calculations are based on more uncertain ionization and recombination data, so differences between the values used by Mazzotta et al. and Arnaud & Rothenflug (1985) can be large. The most important case is the free-bound continuum due to recombination of He III to He II at temperatures around 30 000 K, because Mazzotta et al. (1998) set the He III abundance to zero so that He III free-bound continuum is zero.

The total continuum is affected by the choice of ion abundances by less than 10% at all temperatures larger than $\log T_e = 6.2$, while at lower temperatures it is dominated by the differences found in the free-bound continuum.

4.2. Element abundances

The effects of changes in the adopted dataset of element abundances are larger than those given by different ion abundance datasets, for two reasons. First, differences due to ion abundances are very temperature dependent and are concentrated at temperatures where the ion abundance is far from its peak value: so, even if they are large, their effect on the resulting total continuum emission is normally limited. On the contrary, differences due to element abundances are independent of T and affect the total continuum emission of an element at all temperatures.

The second reason is due to the fact that abundance composition changes in the solar and astrophysical plasmas can be large. As an example, the difference in composition between the solar photosphere and the solar corona is a factor 3 to 4 for the elements with first ionization potential (FIP) smaller than 10 eV (the "FIP effect", i.e. Feldman & Laming 2000, and references therein). This enhancement, present in various degrees also in the coronae of many stars, directly affects the continuum emission.

To check the effects of different element abundance datasets on continuum emission we have compared the results obtained assuming two different datasets, widely used for the solar corona: the photospheric abundances from Grevesse & Sauval (1998), and the coronal abundances from Feldman et al. (1992). The differences between these two datasets concern the elements with FIP < 10 eV, since the Feldman et al. (1992) abundances of such elements are larger than those of Grevesse & Sauval (1998) by factors 3 to 4, to reflect the solar FIP effect.

The effects of element abundances on the free-free continuum are very limited, and the differences between the results obtained with the two datasets are within 15% at the maximum, and in the 5−10% range for wavelengths larger than 20 Å. These limited differences are due to the fact that free-free emission is largely due to ionized hydrogen, whose abundance does not change in the two datasets we adopted.

Differences in the free-bound and two-photon continua are much larger, since in their cases the emission from elements other than hydrogen is very important at nearly all temperatures. Differences in the free-bound continuum for temperatures lower than $\log T_e = 6.4$ are usually moderate, within 30−40% for wavelengths smaller than 20 Å and within 10−50% in the 20−2000 Å range. There are, however, two exceptions: differences up to a factor of three are given at around 1500 Å by the recombination continuum of Si II to Si I at temperatures lower than 15 000 K; and differences up to a factor 1.8 are found at wavelengths shorter than 80 Å for temperatures in the $5.2 \leq \log T_e \leq 6.8$: they are due to the recombination continuum of Mg and Si coronal ions. At temperatures typical of solar flares ($6.6 \leq \log T_e \leq 7.4$), the X-ray continuum below 10 Å is strongly affected by changes in the element abundances. This is due to the fact that H-like and He-like ions of Mg, Si, Ca, Fe and Ni (all with FIP < 10 eV) dominate the free-bound emission at wavelengths shorter than 7 Å: the effects of the two different abundance datasets can be up to a factor three. Differences strongly depend on wavelength, as shown in Fig. 3.

The two-photon emission is also strongly affected by the change in the abundance of the elements with FIP < 10 eV, but the changes occur mostly in the X-ray range. There, differences may be up to a factor two to four, and are strongly wavelength dependent, because of the interplay of the two-photon continuum with elements with FIP < 10 eV and those with FIP > 10 eV. At wavelengths of more than 20 Å, the two abundance datasets provide results in agreement within 20% for all temperatures lower than $\log T_e \leq 6.6$, because the continuum is dominated by elements with FIP > 10 eV. At higher temperatures, however, the two-photon emission from highly ionized elements with FIP < 10 eV starts to dominate and provides differences up to a factor 2−2.5 at $\log T_e = 8.0$. However, at these temperatures the two-photon emission is usually negligible.

The effects on total continuum emission at wavelengths in the 20−2000 Å range are the same as for the free-bound for temperatures lower than 10^6 K, but the rise of the free-free continuum at larger temperatures mitigates the effects of the free-bound emission from recombining Mg and Si coronal ions. At temperatures greater than $\log T_e = 6.6$, the differences decrease to around 5−10%. In the X-rays below 20 Å the interplay of free-free and free-bound continuum causes the differences of the total emission obtained from the two abundance datasets to be greatest in the $6.6 \leq \log T_e \leq 7.4$ temperature range, where recombinations onto elements with FIP < 10 eV causes the total continuum emission to change by factors up to 2. These effects are strongly wavelength dependent, and are found for wavelengths lower than 10 Å; at higher wavelengths recombination of elements with FIP > 10 eV is dominant and differences become smaller. Interestingly, the $6.6 \leq \log T_e \leq 7.4$ temperature range is typical of solar flares, so that a correct choice of the abundance dataset is crucial for any plasma diagnostic use of the X-ray continuum (see Sect. 6). An example of such differences at three

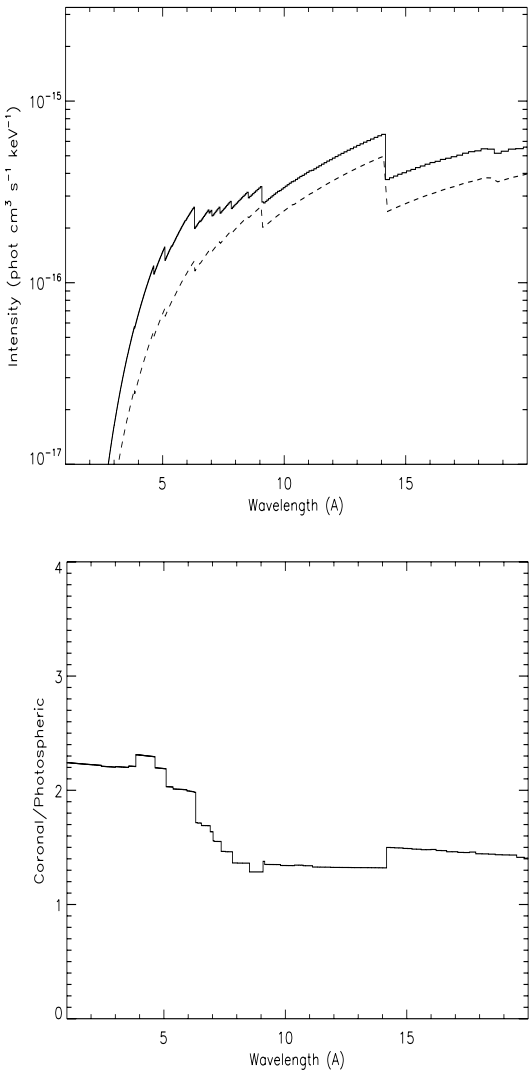

Fig. 3. Differences in the free-bound emission in the 1−20 Å wavelength range due to abundance differences, at $\log T = 7.0$. *Top*: free-bound emissivity, obtained using coronal (full line) and photospheric (dashed line) solar abundances. *Bottom*: ratio between free-bound continua obtained with different abundances.

different temperatures typical of solar flares is shown in Fig. 4, as a function of energy (corresponding to the 1−20 Å range).

5. Comparison of results between CHIANTI and MEWE

The continuum emissivities calculated using CHIANTI and the MEWE approaches have been compared to assess the effects on the results of the different approximations and atomic data within the two codes. In order to be consistent with the MEWE calculations, the CHIANTI continuum emissivities have been calculated adopting the Arnaud & Rothenflug (1985) ion fractions and the Allen (1973) element abundances. Also, a density of 10^{10} cm^{-3} is used for the two-photon continuum, to simulate the low density limit conditions assumed by MEWE. Since the MEWE continuum was optimized between 1−1000 Å, we will restrict the comparison to this wavelength range.

5.1. Free-free continuum

The first thing to note while comparing the free-free continuum as calculated by the CHIANTI and MEWE code is that the latter is much larger than the former at temperatures below 25 000 K, with differences rapidly increasing as the temperature lowers. At 10 000 K, differences rise up to several orders of magnitude, as shown in Fig. 5. Detailed inspection of the software generating the two codes has shown that the MEWE continuum is actually overestimated due to the assumption that the abundance of ionized hydrogen is unity at all temperatures, contrary to the ion abundance values in Arnaud & Rothenflug (1985). The free-free emission at these temperatures is by far dominated by electron-hydrogen interactions so that the abundance of ionized hydrogen, which is unity only at temperatures larger than 25 000 K, is considerable. Once the MEWE free-free continuum is multiplied by the correct values for the abundance of ionized hydrogen, the CHIANTI and MEWE results agree within 30% below 1000 Å.

Differences between the MEWE and CHIANTI free-free continuum models are smoothly varying with wavelength and temperature. Above 25 000 K, the two codes provide results that are largely in agreement. At temperatures up to 10^5 K, the two codes agree within 40%, with the MEWE code being higher than CHIANTI below 100 Å and vice versa at longer wavelengths. At temperatures higher than 10^5 K, the CHIANTI free-free continuum is always larger than MEWE by less than 25%.

5.2. Free-bound continuum

A similar problem in the ionized hydrogen abundance as found in the free-free continuum also affects the MEWE free-bound continuum. At temperatures lower than 25 000 K the free-bound continuum below 912 Å is dominated by the Lyman continuum. The overestimation of the ionized hydrogen abundance in the MEWE model leads to discrepancies between the MEWE and CHIANTI results up to several orders of magnitude. Once the MEWE continuum is multiplied by the correct value of the ionized hydrogen abundance, the two codes agree within 30% below 912 Å (see Fig. 5).

Differences in the free-bound continuum are strongly temperature and wavelength dependent, and their main feature is the presence of a large number of jumps, as shown in Fig. 6 for the 1−6 Å wavelength range. The jumps reflect the different treatment of the free-bound continuum given by the two spectral codes: while in the MEWE code only a very limited number of recombination edges are included in the fit of the Mewe et al. (1986) continuum, the CHIANTI approximation includes them for nearly all the ions in the database. Most of the recombination edges in Fig. 6 give very limited differences (e.g. between 15 Å and 18 Å), being due either to less abundant ions and elements, or to recombinations to excited levels. However, in a few cases such jumps can be substantial. At temperatures where the free-bound continuum is greater than the free-free continuum, the largest differences due to a jump are within 40%; at other temperature regimes such differences can be up to a factor two to three. Also, part of the difference very close to the edge is due to different values of the edge wavelengths $\lambda_{\rm edge}$ in MEWE and CHIANTI.

In general, differences at temperatures between 1 and 10 MK are within 40−50% or smaller in the whole 1−2000 Å range; at very low temperatures ($T_{\rm e} \leq 20\,000$ K) CHIANTI takes into account the important contribution of recombinations to C I, Si I and S I between 1000 Å and 1500 Å that are not included

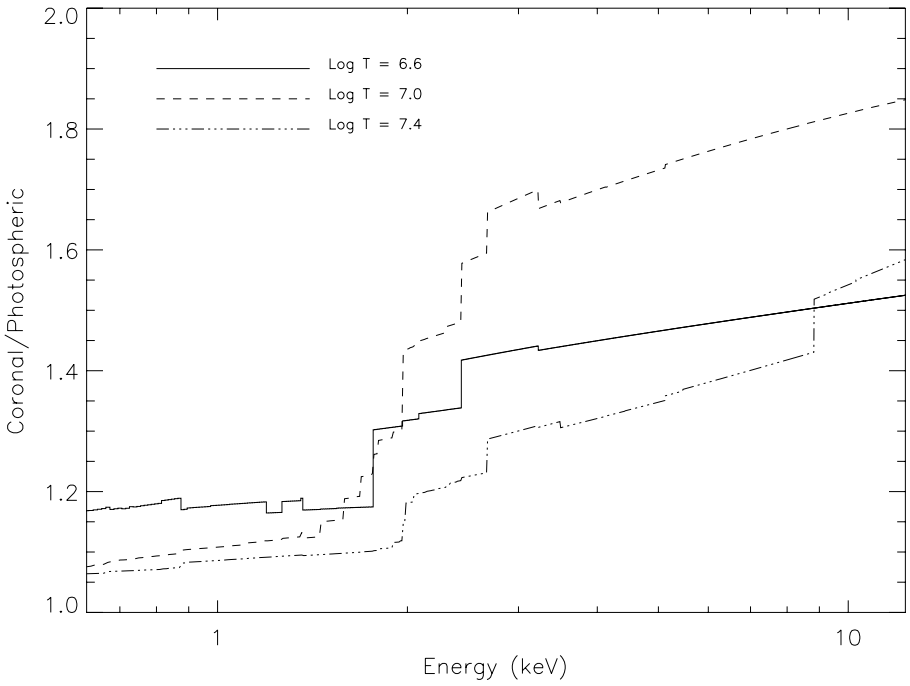

Fig. 4. Ratio between total continuum emission calculated using coronal abundances and photospheric abundances in the X-ray range between 0.6 and 12.3 keV (corresponding to the 1−20 Å wavelength range).

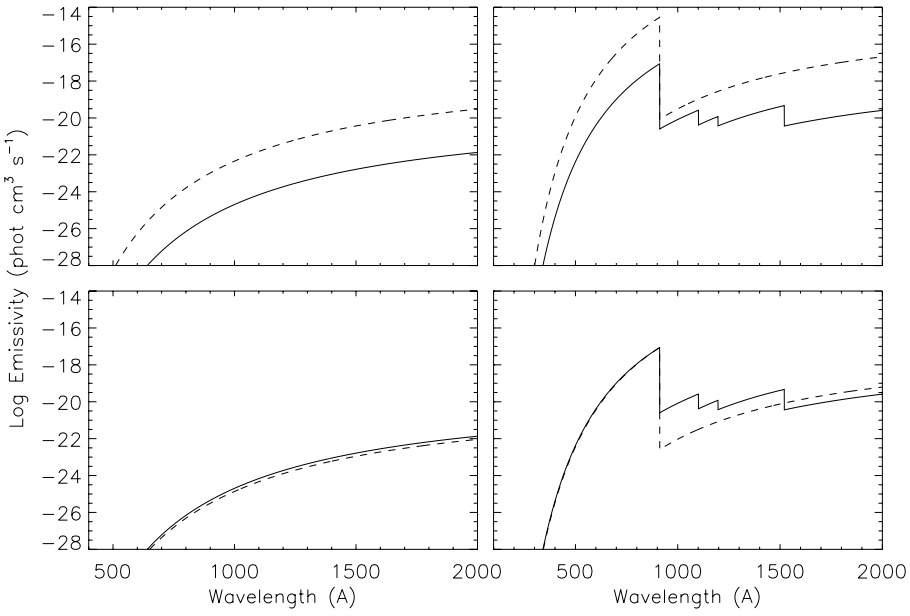

Fig. 5. Comparison of the CHIANTI (full line) and MEWE (dashed line) continuum calculated at T_e = 10 000 K. *Left column*: free-free continuum; *right column*: free-bound continuum. The MEWE continuum in the bottom two panels was multiplied by the H I ion abundance from Arnaud & Rothenflug (1985).

in MEWE. Most of these continua, however, lie outside the wavelength range of the MEWE code (see Fig. 5). Continuum from these ions has been observed by spectrometers operating in the UV.

5.3. Two-photon continuum

Differences in the two-photon emissivities are very large at nearly all temperatures and wavelengths. The first difference lies in the fact that the MEWE continuum is only calculated between 19 Å and 200 Å, where its emissivity is largest, while CHIANTI does not have wavelength restrictions.

In the common wavelength range, two-photon emissivites are largest in the $6.0 \leq \log T_e \leq 6.6$ (T in K) and in this range the two codes provide results in agreement within a factor of two. At low temperatures the MEWE two photon continuum is usually larger than that of CHIANTI below 100 Å, and smaller between 100 Å and 200 Å. At temperatures of $\log T_e > 6.6$ the MEWE two-photon continuum becomes very small very rapidly at all wavelengths, while that of CHIANTI decreases much more slowly.

5.4. Total continuum

The differences in the total continuum, obtained by summing the contributions of free-free, free-bound and two-photon emission, are more moderate than the differences in each individual process. The reason for this lies in the fact that the two-photon

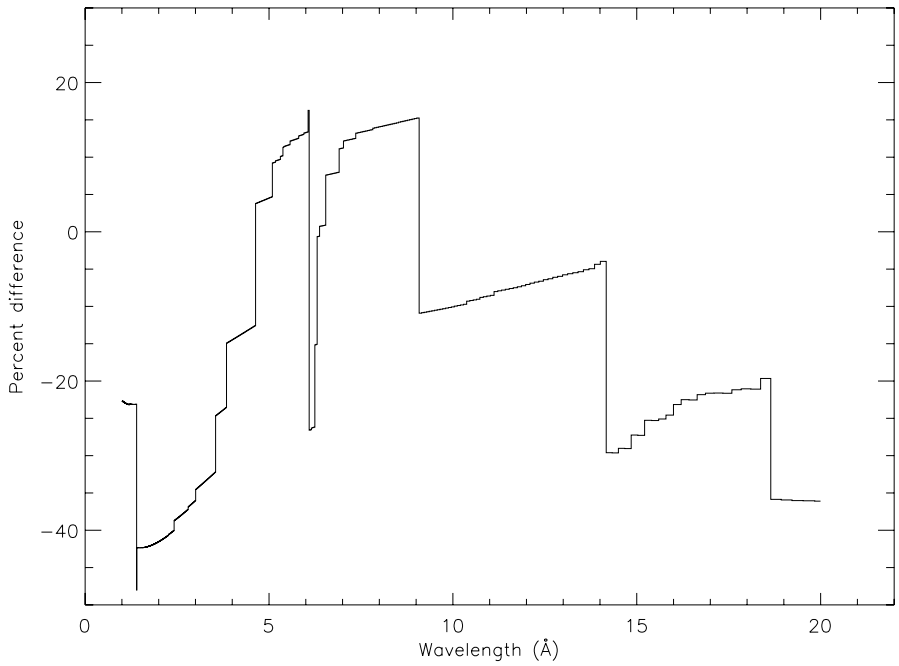

Fig. 6. Percent difference between the CHIANTI and MEWE free-bound continua in the 1−20 Å range. The spectra were calculated at ≃16 MK.

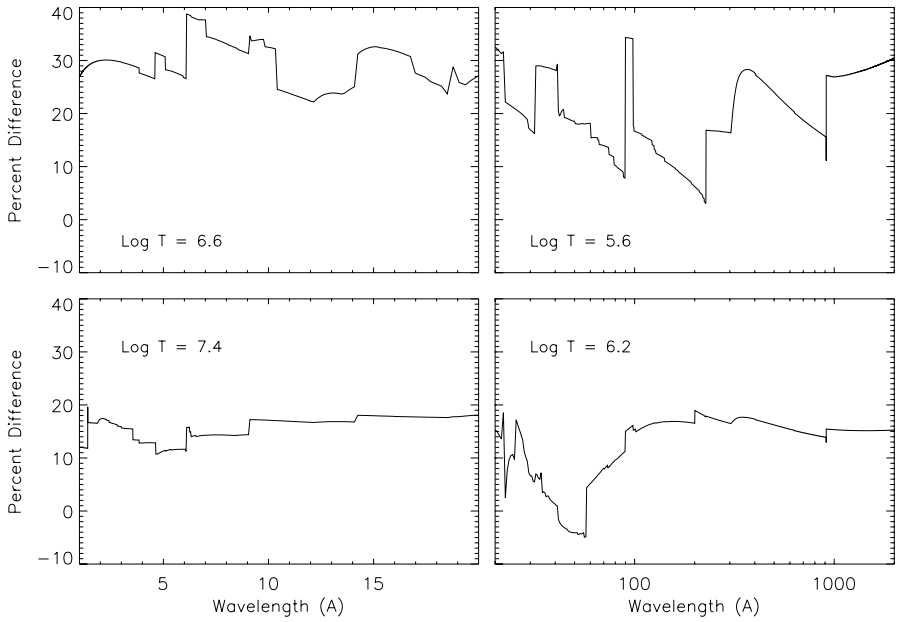

Fig. 7. Percent difference between the CHIANTI and MEWE total continua.

continuum is negligible almost everywhere relative to the other two processes, and the discrepancies at temperatures where differences in the free-bound continuum are larger are mitigated by the fact that free-free emission dominates the total continuum.

Below 20 Å, the CHIANTI continuum is always higher than the MEWE results at all temperatures and wavelengths, but the differences are within 40% in all cases and decrease to 5−20% at temperatures larger than 6 MK, where continuum emission is mostly observed in solar flares. Examples are shown in Fig. 7.

Similar differences are also found at other wavelengths and temperature ranges, with the only exception being $T_e \leq 25\,000$ K where the H I recombination continuum in the MEWE code is overestimated.

6. Plasma diagnostic consequences

6.1. Effects of the X-ray free-bound emission

As discussed in Sect. 3, the X-ray free-bound continuum is not negligible in the 1−10 Å range for temperatures typical of solar and stellar flares.

As an example, Fig. 8 shows the percentage of free-free continuum emission over the total continuum as a function of temperature at three different wavelength ranges. Full lines correspond to calculations carried out assuming coronal element abundances, dashed lines correspond to results obtained with photospheric abundances.

The three wavelengths correspond to regions of the continuum close to the H-like and He-like Ca (3.2 Å) and S (5.0 and

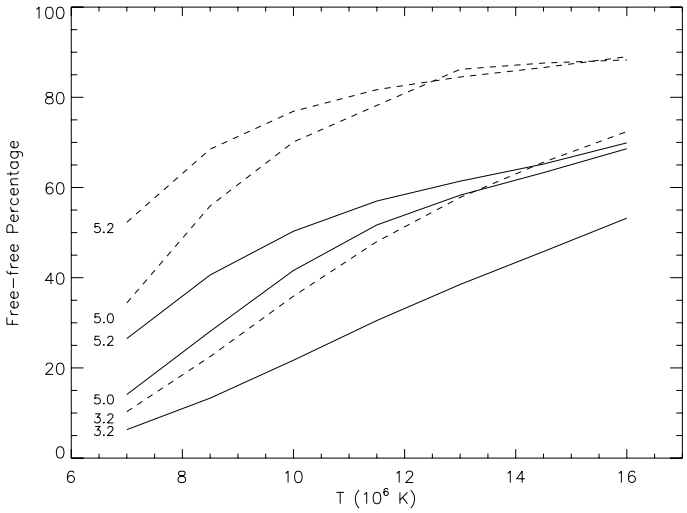

Fig. 8. Percent of free-free radiation in the total continuum at 3.2 Å, 5.0 Å and 5.2 Å. Full line: coronal abundances; dashed line: photospheric abundances.

5.2 Å) ions, routinely observed by the Yohkoh Bragg Crystal Spectrometer (BCS) over its entire operational life. Even in the most conservative case (photospheric abundances and high T) the free-bound continuum contributes at least 10–30% to the total emission. However, element abundances in flares were often found to be coronal: in this case the free-bound contribution is much larger and can be dominant.

Figure 8 clearly shows that the EM and the element abundance values measured from Yohkoh observations using only free-free radiation are likely to be overestimated.

6.2. Effects of element abundances

The dependence of the predicted continuum emission on user-defined parameters may have very important consequences for emission measure and abundance measurements from X-ray spectra of flares, where continuum emission is strong and routinely observed. The effect of ion abundances on the total continuum emission below 20 Å is negligible, being around 10%. Also, the approximations in the two spectral codes (MEWE and CHIANTI) are of little consequence for plasma diagnostics. On the contrary, the choice of the wrong set of abundances may have serious effects on diagnostic results.

Since the free-bound emission is either larger than, or comparable to the free-free emission below 20 Å at temperatures in the $6.6 \leq \log T \leq 7.4$ range, and the effects of element abundances on the total predicted continuum emission is large (up to a factor two), the use of the wrong set of abundances (i.e. photospheric abundances for plasmas whose composition is coronal) leads to an underestimation or overestimation of the continuum emissivity. Such errors are directly propagated to the continuum-based estimates of the emission measure of the emitting plasma (and hence to plasma volume, filling factor and radiative losses), and of the absolute abundance measurements carried out using line-to-continuum ratios.

These problems cannot be avoided when using the MEWE code, since its continuum emission is calculated through formulae fitted on continuum radiation based on the element abundances from Allen (1973), very similar to the abundances of the solar photosphere. Since abundances have been found to be coronal rather than photospheric in many flares (i.e. Phillips et al. 2003; Feldman et al. 2003, 2004), the use of the MEWE code may lead to incorrect results.

Figure 8 shows, for example, that an incorrect choice of element abundances leads to huge changes to the total continuum emission at 3.2, 5.0 and 5.2 Å spectral regions observed by Yohkoh. For this reason, EM and abundance measurements from Yohkoh observations obtained using the MEWE code should be treated with caution as they might be inaccurate.

7. Summary

In the present study we investigated the free-free, free-bound and two-photon emission from optically thin plasmas in the 1–2000 Å range. We compared continuum calculations from two widely used spectral codes adopting different data and approximations to assess the effects of their differences on the predicted emission. We investigated the effects of user-defined parameters such as ion and element abundances on the resulting continuum emission and their effects on plasma diagnostics. We also investigated the relative importance of the different kinds of continuum as a function of wavelength and temperature, and their consequences for plasma diagnostics.

We found that results from the two different spectral codes are within 40% at all temperature ranges, and in most cases within 15–20% thus showing that different approximations and atomic data have limited effects on the overall accuracy of predicted continuum emission. An error was found in the Mewe et al. (1986) continuum calculations available in *SolarSoft* for the H I free-bound continuum at temperatures lower than 25 000 K, leading to differences of more than one order of magnitude.

Ion abundances usually have small effects (within 10%) on the continuum emission from plasmas with temperature larger than $\log T_e = 6.2$, while larger effects are found whenever recombination continuum from ions with fractional abundance lower than 1×10^{-3} dominates the total continuum.

Element abundances have little effect on the free-free continuum, but are a crucial parameter for the calculation of the free-bound continuum. Their effect on the total continuum is strongly dependent on temperature and wavelength.

We also found that element abundances are an important factor to be taken into account when using X-ray spectra for emission measure and absolute abundance measurements from flares with temperatures in the $6.6 \leq \log T_e \leq 7.4$. This is because the free-bound emission is not negligible below 10 Å in that temperature range. As a result, diagnostic results obtained using the Mewe et al. (1986) continuum available in *SolarSoft* for plasma diagnostics from X-ray spectra of flares needs to be treated with caution, as element abundances are fixed and calculations are carried out adopting a set of solar photospheric abundances that may be significantly different from the real abundances in the flare plasma.

Acknowledgements. The work of Enrico Landi is supported by the NNH06CD24C, NNG04ED07P and other NASA grants. The author thanks Drs. H. Hudson, A. Caspi, K. J. H. Phillips and J. Sylwester for stimulating discussions.

References

Allen, C. W. 1973, Astrophysical Quantities (London: the Athlone Press)
Arnaud, M., & Rothenflug, R. 1985, A&AS, 60, 425

Curdt, W., Brekke, P., Feldman, U., et al. 2001, A&A, 375, 591
Dere, K. P., Landi, E., Mason, H. E., Monsignori Fossi, B. C., & Young, P. R. 1997, A&AS, 125, 149
Dere, K. P., Landi, E., Young, P. R., & Del Zanna, G. 2001, ApJS, 134, 331
Feldman, U., & Laming, J. M. 2000, Phys. Scr., 61, 222
Feldman, U., Mandelbaum, P., Seely, J. L., Doschek, G. A., & Gursky, H. 1992, ApJS, 81, 387
Feldman, U., Landi, E., Doschek, G. A., Dammasch, I., & Curdt, W. 2003, ApJ, 593, 1226
Feldman, U., Dammasch, I., Landi, E., & Doschek, G. A. 2004, ApJ, 609, 439
Feldman, U., Landi, E., & Laming, J. M. 2005, ApJ, 619, 1142
Grevesse, N., & Sauval, A. J. 1998, Sp. Sci. Rev., 85, 161
Gronenschild, E. H. B. M., & Mewe, R. 1978, A&AS, 32, 283
Itoh, N., Sakamoto, T., & Kusano, S. 2000, ApJS, 128, 125
Karzas, W. J., & Latter, R. 1961, ApJS, 6, 167
Landi, E., Landini, M., Dere, K. P., Young, P. R., & Mason, H. E. 1999, A&AS, 135, 339
Landi, E., Del Zanna, G., Young, P. R., et al. 2006, ApJS, 162, 261
Landi, E., Feldman, U., & Doschek, G. A. 2007, ApJ, 659, 743
Landini, M., & Monsignori Fossi, B. C. 1990, A&AS, 82, 229
Lin, R. P., Dennis, B. R., Hurford, G. J., et al. 2002, Sol. Phys., 210, 3
Mazzotta, P., Mazzitelli, G., Colafrancesco, S., & Vittorio, N. 1998, A&AS, 133, 403
Mewe, R., Lemen, J. R., & van den Oord, G. H. J. 1986, A&AS, 65, 511
Phillips, K. J. H. 2004, ApJ, 605, 921
Phillips, K. J. H., Sylvwester, J., Sylwester, B., & Landi, E. 2003, ApJ, 589, L113
Phillips, K. J. H., Chifor, C., & Dennis, B. R. 2006, ApJ, 647, 1480
Rybicki, G. B., & Lightman, A. P. 1979, Radiative processes in Astrophysics (New York: Wiley)
Sutherland, R. S. 1998, MNRAS, 312, 813
Sylwester, J., Gaicki, I., Kordylewski, Z., et al. 2005, Sol. Phys., 226, 45
Sylwester, J., Sylwester, B., Phillips, K. J. H., et al. 2006, Adv. Sp. Res., 38, 1490
Verner, D. A., & Yakovlev, D. G. 1995, A&AS, 109, 125
Young, P. R., Del Zanna, G., Landi, E., et al. 2003, ApJS, 144, 135
Wilhelm, K., Curdt, W., Marsch, E., et al. 1995, Sol. Phys., 162, 189